

Article

Variability of Glacier Velocity and the Influencing Factors in the Muztag-Kongur Mountains, Eastern Pamir Plateau

Danni Huang ¹, Zhen Zhang ² , Ling Jiang ^{1,*}, Rui Zhang ^{3,4} , Yijie Lu ², AmirReza Shahtahmassebi ¹ and Xiaoli Huang ¹

¹ College of Geographic Information and Tourism, Chuzhou University, Chuzhou 239000, China

² School of Spatial Informatics and Geomatics, Anhui University of Science and Technology, Huainan 232001, China

³ Faculty of Geosciences and Environmental Engineering, Southwest Jiaotong University, Chengdu 611756, China

⁴ State-Province Joint Engineering Laboratory of Spatial Information Technology for High-Speed Railway Safety, Southwest Jiaotong University, Chengdu 611756, China

* Correspondence: ling.jiang@chzu.edu.cn; Tel.: +86-25-15605503315

Abstract: Glacier velocity is the key to understanding the nature of glaciers. Its variation plays an important role in glacier dynamics, mass balance, and climate change. The Muztag-Kongur Mountains are an important glacier region in the Eastern Pamir Plateau. Under the background of global warming, the glacier velocity variation has been widely considered, but details of the inter-annual and intra-annual changes have not been clear. In this study, we explored the inter-annual and intra-annual variations in the glacier velocity from 1990 to 2021, and the influencing factors, based on Landsat images, Inter-Mission Time Series of Land Ice Velocity and Elevation (ITS_LIVE), and Karakoram Highway (KKH) data product analysis. The results showed the following: (1) the glacier velocity has increased since 1990, and significant growth occurred in 1995–1996. (2) A transverse profile of two typical glaciers was used to analyze the monthly variation in glacier velocity during the year. The peaks of monthly velocity occurred in May and August. (3) Since 1990, the inter-annual precipitation has increased, and the temperature increase slowed down from 2000 to 2013. The trend of inter-annual glacier velocity variation was consistent with that of the precipitation. The glacier velocity peaked in 1996/1997 due to increased precipitation in 1995. The glacier velocity over the year was consistent with the monthly precipitation trends, which indicates that precipitation has a significant influence on the change in glacier velocity. (4) In addition to temperature and precipitation, the glacier velocity variation was moderately correlated with the glacier size (length and area) and weakly correlated with the slope. The spatial distribution of glaciers shows that the spatial heterogeneity of glaciers in the Muztag-Kongur Mountains is affected by the westerly circulation. The long-term glacier velocity variation research of the Muztag-Kongur Mountains will contribute to a better understanding of glacier dynamics within the context of climatic warming, and the different influencing factors were analyzed to further explain the glacier velocity variation.

Keywords: Muztag-Kongur Mountains; glacier velocity; glacier velocity variation



Citation: Huang, D.; Zhang, Z.; Jiang, L.; Zhang, R.; Lu, Y.; Shahtahmassebi, A.; Huang, X. Variability of Glacier Velocity and the Influencing Factors in the Muztag-Kongur Mountains, Eastern Pamir Plateau. *Remote Sens.* **2023**, *15*, 620. <https://doi.org/10.3390/rs15030620>

Academic Editor: Ulrich Kamp

Received: 18 December 2022

Revised: 17 January 2023

Accepted: 18 January 2023

Published: 20 January 2023



Copyright: © 2023 by the authors. Licensee MDPI, Basel, Switzerland. This article is an open access article distributed under the terms and conditions of the Creative Commons Attribution (CC BY) license (<https://creativecommons.org/licenses/by/4.0/>).

1. Introduction

Glaciers are sensitive indicators of climate change and an important freshwater resource [1]. As an important parameter of glacier dynamics, glacier velocity is a key factor to understand the nature of glaciers. It can not only respond to the mass balance variations, but also reflects the dynamic information of the glacier surface [2,3]. With climate change, glacier movement controls the change of ice transport, which in turn affects the length, area, mass balance, and thickness of glaciers [4]. Therefore, investigating glacier velocity is a crucial parameter in analyzing glacier dynamics, glacier mass balance, and glacier change.

Methods for determining glacier velocity include field measurements and remote sensing techniques [5]. In the first method, measurement stakes are installed on the glacier, and the moving distance of the stakes is measured to obtain the glacier flow velocity. This method is highly accurate, but the placement and monitoring of the measurement stakes are labor-intensive and costly due to the complex terrain; therefore, it is not widely used [6]. Remote sensing techniques are the primary method to assess glacier velocity due to the advantages of large data storage and a wide monitoring range [7,8]. Remote sensing methods for extracting glacier velocity include radar differential interferometry, Synthetic Aperture Radar (SAR) offset tracking, and optical remote sensing monitoring [9]. It is difficult to obtain high-coherence images from radar differential interferometry in complex terrains, such as mountain glaciers. Thus, this method is not commonly used to obtain the velocity of mountain glaciers [10]. The SAR offset tracking method is not affected by clouds and fog, but it is only suitable for short-term glacier velocity extraction [5,11]. Optical remote sensing monitoring is affected by the weather, but there is a large historical image archive, especially Landsat data. Therefore, this method is more suitable because of the long time-series data available [12].

Due to global warming, most glaciers are thinning and melting, and are in a state of retreat and mass loss [13]. However, the glaciers in the Pamir Plateau are relatively stable or have advanced, exhibiting a slight positive mass balance, which is referred to as the 'Pamir-Karakoram anomaly' phenomenon [14–16]. In particular, the glaciers of the Eastern Pamir Plateau became thicker in the early 21st century, with large differences between individual glaciers [15,17,18]. Increased temperatures, westerly circulation, and positive and negative cyclonic effects caused this systematic regional heterogeneity [19]. The Muztag-Kongur Mountains, which contain 52% of the glaciers in the Eastern Pamir Plateau, is an important glacier gathering area. The study of its changes may increase our understanding of glacier changes in the entire Eastern Pamir Plateau. Most researchers recognize that glacier changes occur in the region through area changes and mass balance. With the increase in temperatures, the glacier area shrank by $1.9 \pm 0.2\%$ between 1971 and 2014, and a slight expansion was detected from 2009 to 2014 [20]. Studies have shown that the Muztag-Kongur Mountains are in the positive mass balance region of the mass balance transition zone due to the increasing westerly circulation. Individual glaciers are relatively heterogeneous [17,18]. In general, glacier movement is accompanied by material transfer, which affects the glacier mass balance [20]. Glaciers maintain a dynamic equilibrium by moving matter from the accumulation area to the ablation area [21]. Under the same climatic background, the heterogeneity of glacier mass balance can be reflected in glacier dynamics, and then reflected by glacier velocity [2]. Therefore, it is of great significance to study the change of glacier velocity. However, few studies have analyzed glacier velocity.

Several researchers have studied the velocity changes of the Muztag-Kongur Glacier. For example, three typical glaciers in the Kongur Mountains and the Kuksai glacier were analyzed in detail [22,23]. A wavelet-based topographic effect compensation algorithm was used to improve the accuracy of mountain glacier velocity extraction, using the Muztag Mountain Glacier as a case study [24]. These studies focused on velocity changes of typical glaciers, but there is a lack of research on glacier velocity in the entire region. One study of glaciers in the High Mountain Asia (HMA) region showed a decrease in the inter-annual velocity of glaciers in the Pamir region from 2000 to 2017. They analyzed High Mountain Asia (HMA) glacier changes, but the spatial trends and velocity changes of glaciers in the interior of the Pamir Plateau remain unclear [21]. In addition, glacier surge is a special kind of glacier flow [25]. A period of glacier surging is generally accompanied by a sudden increase and decrease in glacier velocity. Several researchers have analyzed the characteristics of glacier surges using glacier velocity. For example, in the case of the 2015 Karayaylak Glacier surges on the northern side of the Kongur Mountains, Landsat images were used to analyze the velocity of the glacier before and after the surge, and to obtain the start and end time of the surge [26]. Some researchers have conducted glacier analysis based on changes in velocity and volume, and proposed a 100-year cycle [27].

The surge mechanism of the Karayaylak Glacier was inferred based on velocity changes and hydrological conditions before and after the surge [28]. Therefore, glacier velocity can provide new insights into the mechanism of glacier surges.

This study used remote sensing data to extract the inter-annual and intra-annual glacier velocity variation of the Muztag-Kongur glaciers. The spatial distribution of glacier velocity was obtained, and the inter-annual and intra-annual glacier velocity were determined to understand the response of glacier velocity to climate change and explore the reasons for heterogeneous glacier changes under climate change.

We used Landsat image data and the frequency-domain cross-correlation algorithm to extract the inter-annual glacier velocity. Inter-Mission Time Series of Land Ice Velocity and Elevation (ITS_LIVE) data were used as supplemental data to derive the inter-annual glacier velocity. The temperature and precipitation data were incorporated to analyze glacier velocity changes in the Muztag-Kongur Mountains from 1990 to 2021. A dataset of glacier surface motions along the Karakoram Highway (KKH, 2015–2016) was used to analyze the monthly velocity changes of typical glaciers during the year. Finally, we comprehensively considered the influence of glacier scale, slope, aspect, and debris cover on glacier velocity.

2. Study Area and Datasets

2.1. Study Area

The study area was the western part of the Taklamakan Desert in the Muztag-Kongur Mountains in the Eastern Pamir Plateau (Figure 1). The area is characterized by crisscrossing ravines and a complex topography. The mountains are oriented northwest–southeast (NW–SE), with an average altitude of more than 7000 m. The climate in this region is strongly influenced by the westerly circulation. The precipitation in the study area is scarce, and the temperature differences are large. Solid precipitation may exist in high altitude areas throughout the year [29]. The extremely high altitude and dry–cold climate are conducive to abundant glaciers in the Muztag-Kongur Mountains area. The results of the China second glacier inventory indicated there were 504 glaciers in the Muztag-Kongur Mountains, with an area of 1009.74 km² [30]. Due to the westerly circulation, the glaciers on both sides of the mountains are relatively large. There are 37 glaciers larger than 5 km², with a total size of 678.8 km². The study area contains the three largest glaciers in the Eastern Pamir Plateau (Figure 1b): the Karayaylak Glacier (115.37 km²), Qimugan Glacier (108.75 km²), and Kuksai Glacier (77.73 km²).

2.2. Datasets

We used data from multiple sources acquired between 1990 and 2021, including Landsat imagery, Advanced Spaceborne Thermal Emission and Reflection Radiometer Global Digital Elevation Model Version 2 (ASTER GDEM V2), ITS_LIVE, and the dataset of glacier surface motion along the KKH [31] (Table 1).

The Landsat series data consists of optical images of the world from 1972 to the present. It covers a long period of time and was the main data source for extracting glacier velocity in this study. We used Level 1T Landsat images. These images have been orthorectified by the United States Geological Survey (USGS) using the Global Land Survey 2005 (GLS2005) global land control point system. The correction accuracy is about half a pixel, and some images have accuracies of 1/6 to 1/10 of a pixel [32]. Therefore, we only performed registration. We used the following principles to select images: (1) we chose images with few clouds and low snow reflectivity to ensure good quality of the image and (2) we used images acquired from May to October because the glacier was melting, and there was less snow cover, so it was less affected by snow accumulation [33]. In addition, the start month and end month for extracting the annual glacier velocity were selected as the same month of the following year as far as possible [33,34]. This is because the glacier surface characteristics of the same months were similar and easy to match. The time interval was 365 ± 32 days, or approximately 1 year. However, in some cases, the image quality of

the end month was low, and we had to select an image from the previous month or the following month. We processed 14 Landsat 5 Thematic Mapper (TM) images (Band 3) and 17 Landsat Operational Land Imager (OLI) images (Band 8). After 2003, the Landsat 7 ETM+ sensor was damaged, and there were few Landsat 5 images available for the Eastern Pamir Plateau; thus, we used the ITS_LIVE data from 2000 to 2013 as a supplement. Because of the different data sources, we divided the Muztag-Kongur Mountain glaciers into three periods for velocity analysis. These three periods were 1990–1999, 2000–2012, and 2013–2021.

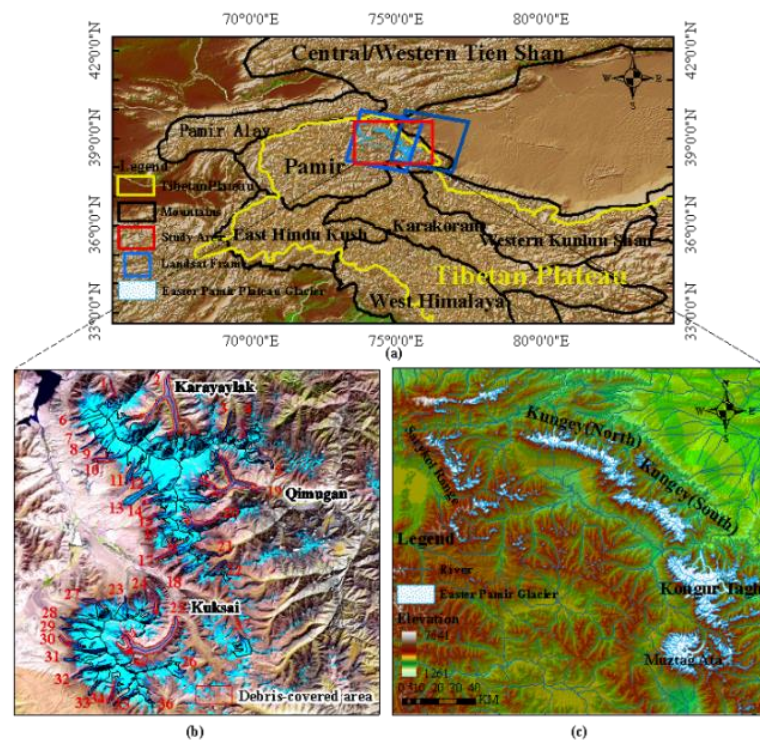


Figure 1. Study area. (a) The red square is the study area and the blue squares are Landsat scenes. (b) Study area overlaid on a Landsat-8 Operational Land Imager (OLI) false-colored composite image (red = 5, green = 4, blue = 3) acquired on 29 September 2019. It shows the glaciers with an area of more than 5 km² in the Muztag-Kongur Mountains. The red polygons are areas covered by debris on the glacier. (c) Overall distribution of glaciers with respect to the elevation. The coordinates of the study area are between 38°N–39°N and 74°40'E–75°40'E.

The ASTER GDEM V2 data were utilized to extract the glacier length and centerline. ASTER satellite data consists of rich 3D information, fully meeting the application requirements of the cryosphere. In particular, it is not affected by snow penetration [35].

We used ITS_LIVE data from the Making Earth System Data Records for Use in Research Environments (MEaSUREs) project of the National Aeronautics and Space Administration (NASA) (<https://its-live.jpl.nasa.gov/>, accessed on 17 September 2019). This is a glacier data product extracted from Landsat 4, 5, 7, and 8, and contains global glacier velocity and elevation change data from 1985 to 2018. The product uses bands 1–4 from Landsat 4 and 5 and the panchromatic band from Landsat 7 and 8. The missing data in Landsat 7 were supplemented with random data, and local normalization, oversampling, and feature tracking were performed to extract the glacier velocity [36]. The normalized displacement coherence (NDC) filter was used to search for areas that are not successfully matched. The error of the velocity component was corrected, and the velocity was extracted at the sub-pixel level [36,37]. The data resolutions were 120 and 240 m. Only the time-averaged velocity was offered at 120 m resolution. We used the 240 m resolution data in this study. Previous studies have used this data to assess glacier movement in HMA, confirming the applicability of the ITS_LIVE data [21].

Table 1. Remote sensing data used in the present research.

Data Type Parameter	Landsat			ASTER GDEM V2	ITS_LIVE	KKH
	5	7	8			
Spatial Resolution/m	30	15	15	30	120	100
Acquisition Period	1989–1999	1999–2000	2013–2021	2011	2003–2012	2015–2016
Coverage	Path 149, Row 33 Path 150, Row 33			N37E073–N39E075	/	Path 27 Frame 121 Path 27 Frame 117 Path 27 Frame 112
Sensor	TM	ETM+	OLI	/	/	/
Purposes	Inter-annual glacier velocity for 1990–2000 and 2013–2021			Glacier length, centerline	Inter-annual glacial velocity from 2000 to 2013	Monthly average velocity during 2015–2016

A dataset of glacier surface velocity along the KKH was also selected to analyze the intra-annual velocity changes of typical glaciers [31]. The dataset is a continuous glacier velocity product along the KKH from 2015 to 2017, with a temporal span of 12/24 days. The glacier velocity data were derived using the Sentinel-1A Interferometric Wide-Swath (IW) mode and vertically (VV) polarized data. Fine topographic registration, feature matching, offset tracking, and extraction of the distance and azimuth offset were performed. The data were combined with slope information from a digital elevation model (DEM) to calculate the glacier surface velocity [31]. Due to the time continuity and short time interval, these data are suitable for analyzing intra-annual monthly velocity changes. Some researchers have used this data to analyze the characteristics of glacier velocity along the KKH, verifying the applicability of the data [38]. Subsequently, in order to be consistent with the meteorological data, we take the KKH data of 2015–2016 as an example to analyze the change of intra-annual glacier velocity.

In addition, we used the glacier profile version 6 of the Randolph Glacier Inventory (RGI 6.0) data [39]. The aspect, slope, median elevation, and surface debris cover of the glaciers were obtained from RGI 6.0. The temperature and precipitation data were obtained from the Taxkogan meteorological station from 1990 to 2016. All data in this research were in the WGS1984 UTM 43N coordinate system.

3. Methods

The glacier velocity was extracted as follows: (1) pre-processing consisted of image co-registration; (2) the glacier velocity was calculated using the Co-Registration of Optically Sensed Images and Correlation (COSI-Corr) framework [40]; and (3) post-processing including the analysis of the output from the second step. These steps are presented in Figure 2 and are described in the following sections.

3.1. Pre-Processing

The Landsat series data used in this paper were all Level 1T data, which had been orthorectified by the USGS. Therefore, we only performed image co-registration in ENVI software 5.1.

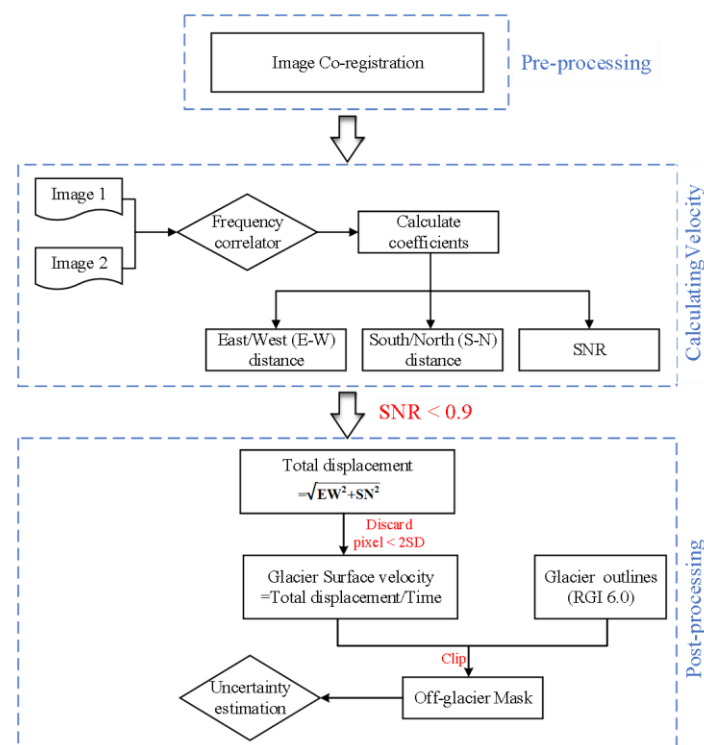


Figure 2. Overview of the research methodology.

3.2. Calculating Glacier Velocity

In order to calculate the glacier velocity, this research utilized the COSI-Corr framework. This framework quantifies the ground deformation of multi-temporal images. COSI-Corr computes the frequency domain phase correlation on two remote sensing images with different time phases. This approach has shown promising results in shadow and snow areas [40], and has been widely used for analyzing glacier velocity [4,28,34].

On the two images, according to the appropriate size of the window and step, the window was moved to a certain search area for cross-correlation calculation. The two points with the largest correlation coefficients in the window were the corresponding points. By calculating the offset between the corresponding points, the displacement of the overlapping area of the two images in the interval time was obtained. The results included East–West (EW) and North–South (NS) displacements and the signal-to-noise ratio (SNR). The total displacement was calculated by the EW and NS displacements, and the glacier velocity was obtained according to the time interval.

The initial and final window sizes for calculating the correlation coefficients in the COSI-Corr framework are typically 128 and 32, respectively. In calculating the glacier velocity, only the velocity pixels with $SNR < 0.9$ should be considered, to eliminate the influence of clouds and shadows [28,34]. These values are empirically determined, so must be selected carefully.

We only analyzed the velocity on the ablation area of the glaciers and, using the automatic method of extracting the glacier centerline [41,42], established a 200 m buffer zone around the centerline of the glacier. This is a plug-in that can be inserted into ArcGIS 10.7. According to the accuracy evaluation, the comprehensive accuracy of the method was 94.34%. The distance from the highest to the lowest point along the centerline was defined as the glacier length [41]. In order to ensure the reliability of the velocity results, we removed the pixels with glacier velocities larger than two standard deviations [35].

Glacier surges may have subtle impacts on the multi-year average velocity [35]. Therefore, the ITS_LIVE data were used to remove the glacier velocity data for two years (2013–2017) before and after the Karayaylak surge year (2015). The obtained results showed a multi-year average velocity of $6.23 \text{ m} \cdot \text{a}^{-1}$. The results were not substantially different

from those from 1989 to 2018 ($6.56 \text{ m} \cdot \text{a}^{-1}$). Ultimately, we did not remove these data from the subsequent analysis of the velocity of the Muztag-Kongur Mountain glaciers.

In this research, we used ENVI 5.1 (Harris Geospatial SolutionsTM, Boulder, CO, USA) to implement the COSI-Corr framework. This is an ENVI plugin, and was released by the California Institute of Technology (Pasadena, CA, USA) in 2015 [40].

3.3. Post-Processing

We utilized off-glacier areas for accuracy assessment. It was assumed that these areas were stable, without displacements. The error of the glacier area could be assessed by the off-glacier area [38,43], which can be expressed as:

$$e_{off} = \sqrt{SE^2 + MED^2} \quad (1)$$

where e_{off} is the displacement error of the off-glacier area; MED is the mean displacement; and SE is the standard error of the mean displacement, which can be expressed as:

$$SE = \frac{STDV}{\sqrt{N_{eff}}} \quad (2)$$

where $STDV$ is the standard deviation of the mean displacement of the off-glacier area and N_{eff} is the number of effective pixels that remove the auto-correlation effect, which can be expressed as:

$$N_{eff} = \frac{N_{total} \times PS}{2D} \quad (3)$$

where N_{total} is the number of pixels in the off-glacier area; PS is the pixel resolution; and D is the spatial autocorrelation distance that removes the autocorrelation effect. This distance is generally 20 times the pixel resolution [44]. The uncertainty of the velocity results is shown in Figure 3.

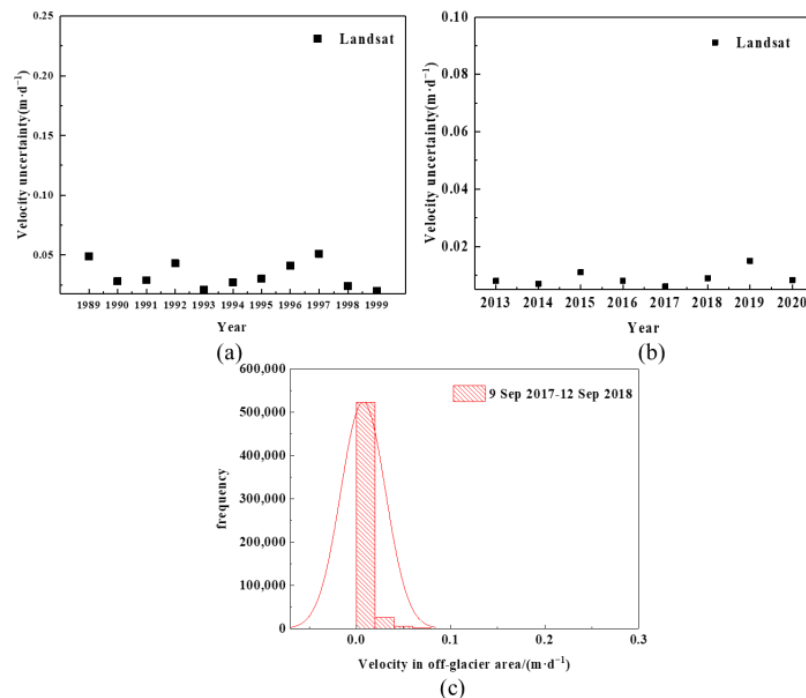


Figure 3. Off-glacier area error. (a,b) Glacier velocity uncertainty between pairs of Landsat images; (c) example of the velocity distribution in an off-glacier area.

We used linear regression to calculate the correlations between the glacier velocity and individual topographic factors and glaciological characteristics, including the area, length, slope, debris cover, and median elevation of the glacier.

4. Results

4.1. Accuracy Assessment

Figure 3 shows the velocity uncertainty result of the Landsat imagery. The error in the off-glacier area ranged from $0.008 \text{ m}\cdot\text{d}^{-1}$ to $0.049 \text{ m}\cdot\text{d}^{-1}$ during 1989–1999, and from $0.008 \text{ m}\cdot\text{d}^{-1}$ to $0.15 \text{ m}\cdot\text{d}^{-1}$ from 2013–2021.

4.2. Spatial Distribution of Glacier Velocity

Table 2 lists the annual average velocity results of the Muztag-Kongur Mountain glaciers from 2013 to 2021. The uncertainty in the glacier velocity was $0.0095 \text{ m}\cdot\text{d}^{-1}$, and the median velocity was $0.0276 \text{ m}\cdot\text{d}^{-1}$ for glaciers with an area of 5 to 10 km^2 and $0.0359 \text{ m}\cdot\text{d}^{-1}$ for glaciers larger than 10 km^2 , suggesting that the velocity was higher for large glaciers than for small glaciers.

Table 2. Parameters of glaciers larger than 5 km^2 in the Muztag-Kongur Mountains.

No.	Glacier	Aspect	Area/ (km^2)	Length/ (km)	Slope/ ($^\circ$)	Debris Cover/ (%)	Median Elevation/ (m)	2013–2021 Average Velocity/ ($\text{m}\cdot\text{d}^{-1}$)
1	Karayaylak	NE	11.56	8.85	32.85	12.13	5322.2	0.014535
2		NE	115.16	18.00	31.92	22.26	4558.6	0.046191
3		NE	9.93	8.56	29.70	25.67	4519.4	0.027377
4		N	13.90	6.90	30.80	14.39	4749.2	0.030915
5		E	9.35	7.90	24.32	26.67	4606.8	0.029064
6		W	5.57	6.72	27.01	11.66	5887.2	0.026799
7		NE	7.78	7.85	27.82	0.00	6118.1	0.031815
8		SW	9.03	9.35	24.91	0.00	6121.0	0.018302
9		W	6.90	6.92	29.79	5.24	6034.5	0.030153
10	Guldauban	SW	17.21	8.79	30.02	13.26	5716.4	0.035782
11		SW	14.09	8.51	31.66	0.63	5797.8	0.041576
12		SW	7.16	7.50	28.19	0.00	5484.9	0.051413
13		SW	44.79	14.74	24.05	0.00	5543.6	0.049974
14		W	10.36	8.53	28.44	11.66	5613.2	0.065656
15		W	10.17	6.46	29.75	4.26	5413.3	0.024239
16		NW	8.31	4.98	25.54	2.63	5333.6	0.027900
17		SW	22.95	11.00	23.02	14.55	5165.9	0.030590
18		NW	5.02	4.42	22.75	15.84	5117.3	0.014578
19	Kuksai	SE	108.75	21.33	27.72	25.15	4640.9	0.049217
20		E	26.47	13.89	27.79	23.69	4858.1	0.028345
21		E	8.44	6.33	23.45	35.25	4823.7	0.015233
22		NE	6.88	4.92	23.60	40.63	4682.2	0.015129
23		NE	7.88	12.29	29.70	2.80	5057.3	0.044083
24		NE	12.76	9.83	23.02	17.43	4951.4	0.023283
25		E	77.73	21.10	24.69	31.55	4913.5	0.059232
26		SE	6.54	4.85	14.35	0.00	5148.4	0.013641
27		N	9.16	14.56	31.53	23.00	5439.0	0.020103
28	Kematulega	NW	9.25	9.68	29.69	0.00	6059.4	0.040873
29		W	7.25	17.00	24.99	0.00	6597.1	0.053000
30	Kalaxiong	W	19.92	9.75	29.62	9.78	5806.5	0.046551
31		W	5.77	8.23	24.05	0.00	5625.9	0.048126
32	Kaskulak	W	15.20	10.90	31.64	0.98	5954.5	0.023581
33		SW	6.66	6.36	31.61	0.00	5783.7	/
34	Kuokluosele	SW	19.89	9.42	25.92	7.49	5474.1	/
35		W	7.95	7.72	29.66	17.70	5363.9	/
36		E	5.23	5.86	28.21	0.00	5093.3	/
37		NE	9.90	6.75	17.57	0.00	5010.5	0.019524

Figure 4 shows the parameters and velocity of the Muztag Mountain glaciers (No. 1–22) and the Kongur Mountain glaciers (No. 23–37). We did not have data for glaciers No. 33–36. The average velocity of glaciers in the Muztag-Kongur Mountains from 2013 to 2021 was $0.0338 \text{ m} \cdot \text{d}^{-1}$. The velocity differed significantly for different glaciers; the maximum velocity was five times that of the minimum velocity, and the standard deviation was $0.0139 \text{ m} \cdot \text{d}^{-1}$. The glacier on the western slope of the Muztag Mountains (No. 14) had the fastest velocity ($0.0657 \text{ m} \cdot \text{d}^{-1}$), whereas a glacier on the Kongur Mountains (No. 26) had the slowest velocity ($0.0136 \text{ m} \cdot \text{d}^{-1}$).

We investigated 37 glaciers with areas larger than 5 km^2 from 2013 to 2021, because the small glaciers had large velocity differences [21]. Table 2 lists the parameters of glaciers larger than 5 km^2 . Table 2 shows that the glacier velocity was generally higher on the western slopes (W/SW/NW) than on the other slopes (E/SE/NE/N) (Table 2). Except for the surge glaciers, the median glacier velocity was $0.038 \text{ m} \cdot \text{d}^{-1}$ on the western slopes (W), $0.036 \text{ m} \cdot \text{d}^{-1}$ on the SW/NW slopes, and $0.029 \text{ m} \cdot \text{d}^{-1}$ on the other slopes (E/SE/NE/N) for the remaining 16 glaciers. These results indicate that the glacier velocity was higher on western slopes than on eastern slopes, in agreement with the existing research results [45]. The effect of different influencing factors on glacier velocity are discussed in Section 5.

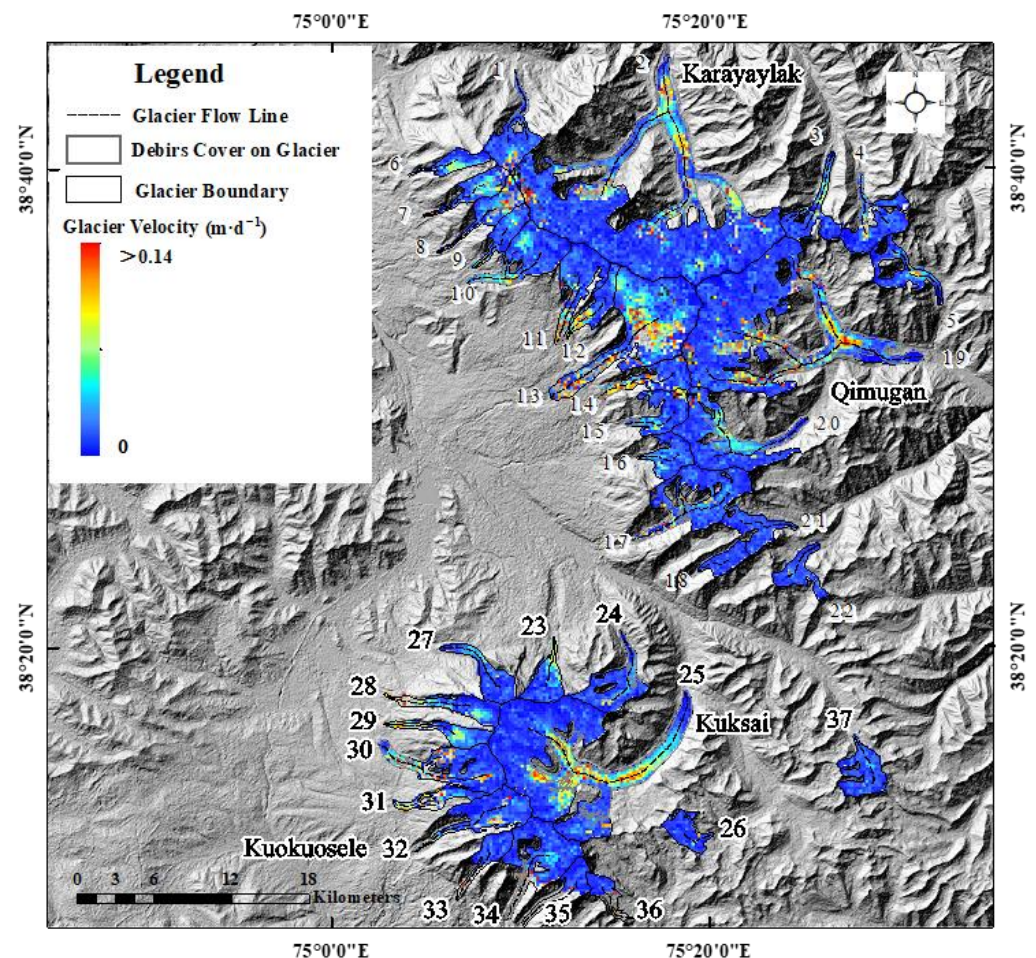


Figure 4. Velocity distribution of glaciers ($>5 \text{ km}^2$) in the Muztag-Kongur Mountains from 2013 to 2021.

4.3. Change in Inter-Annual Glacier Velocity

The velocity changes of the Muztag-Kongur Mountain glaciers are shown in Figure 5.

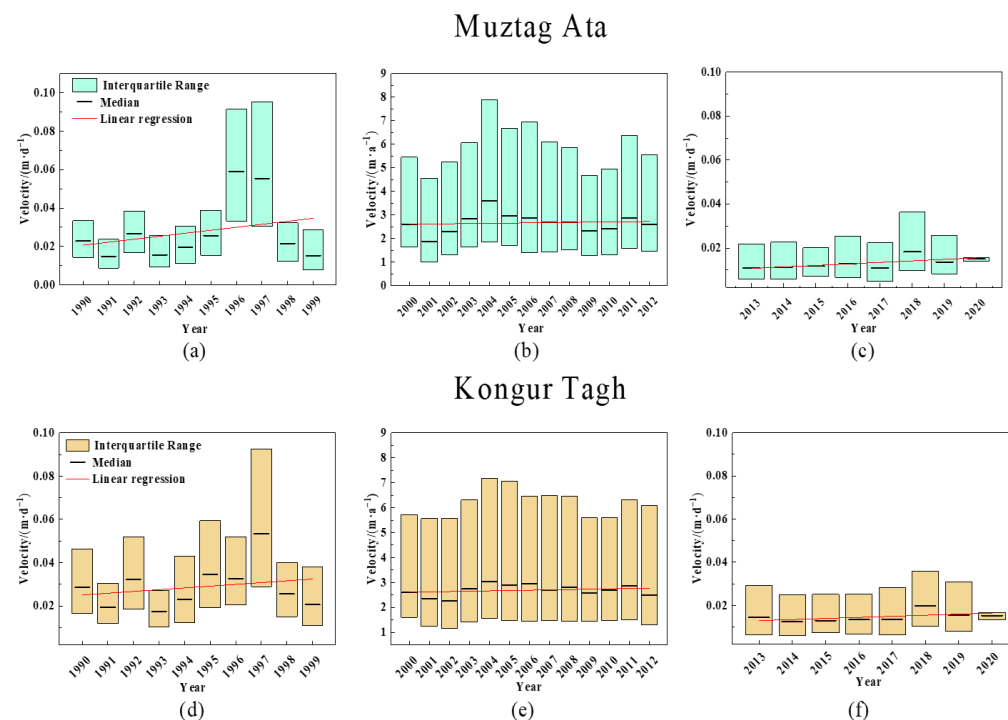


Figure 5. Inter-annual glacier velocity in the Muztag Mountains in (a) 1990–1999, (b) 2000–2012, and (c) 2013–2020, and in the Kongur Mountains in (d) 1990–1999, (e) 2000–2012, and (f) 2013–2020.

Figure 5 shows the median, quartile difference, and trend of glacier velocity in the Muztag-Kongur Mountains [21]. The median and quartiles provide information on the distribution and trends of glacier velocity. The glacier velocity in the Muztag and Kongur Mountains accelerated from 1990 to 1999 (the average increase was 4.79% and 6.35%, respectively). However, the glacier velocity showed a slight acceleration from 2000 to 2012 (the average increase was 1.44% and 0.87%, respectively). Interestingly, the glacier velocity accelerated rapidly from 2013 to 2020 (the average increase was 7.78% and 2.5%, respectively).

The meteorological data obtained from the Taxkogan meteorological station are shown in Figure 6. The temperature and annual precipitation showed an upward trend from 1990 to 1999 (Figure 6). The temperature decreased slightly, and the annual precipitation increased from 2000 to 2012. The temperature and precipitation increased yearly from 2013 to 2016. The trend of the inter-annual velocity was consistent with the precipitation trend (Figures 5 and 6). The glacier velocity was higher from 1996 to 1997, presumably due to the higher precipitation in 1995. Subsequently, the temperature began to rise, and the glacier velocity increased in the following 1–2 years. The main reason for this phenomenon was that an increase in temperature melts the glacier's surface, and the meltwater flows to the bottom of the glacier through fissures and caves. The glacier meltwater acts as a lubricant and reduces the friction at the bottom of the glacier, increasing glacier velocity [2].

4.4. Change in Intra-Annual Glacier Velocity

The glacier velocity data for Kuksai and Kuokusele were obtained from KKH products for the period of 2015–2017 [31]. They are the No. 25 glacier and No. 34 glacier in Table 2, respectively.

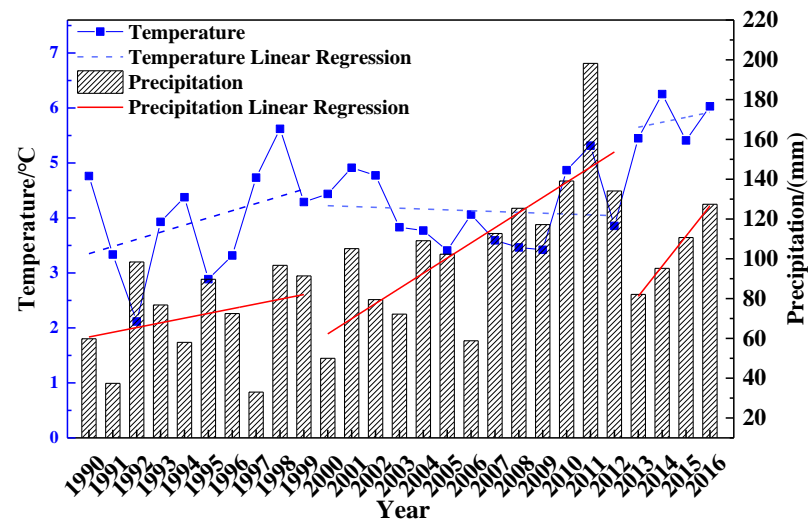


Figure 6. Inter-annual average air temperature and precipitation from 1990 to 2016 at the Taxkogan meteorological station.

4.4.1. Kuksai Glacier

As shown in Figure 7b, the velocity trends of the Kuksai Glacier along the centerline were similar in each month from 2015 to 2016; the velocity was the slowest at the end of the glacier (about $0.013 \text{ m} \cdot \text{d}^{-1}$). The velocity began to accelerate at 5000–6000 m from the end of the glacier (altitude 4289–4336 m). The fastest velocity of $0.15 \text{ m} \cdot \text{d}^{-1}$ was observed at 8000–14,000 m from the end of the glacier (altitude 4421–4666 m). In general, the monthly average glacier velocity increased and decreased in 2015–2016. The highest velocity occurred in June ($0.18 \text{ m} \cdot \text{d}^{-1}$), and the velocity was lower in July than in the adjacent months.

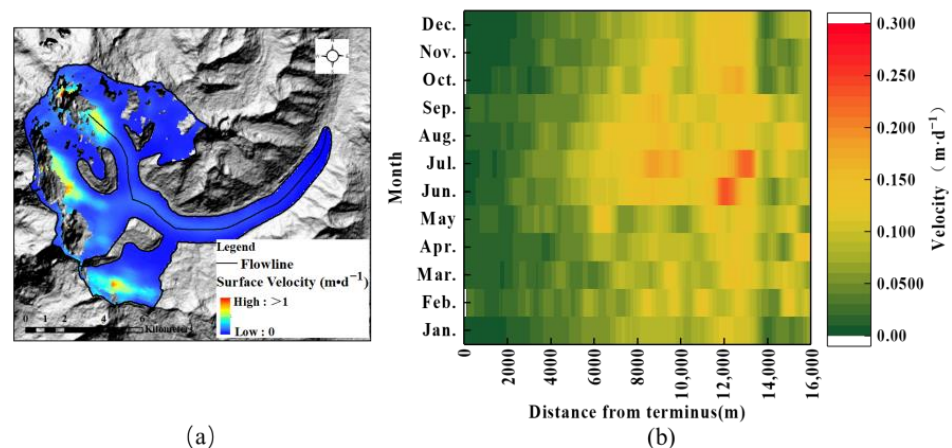


Figure 7. Changes in the monthly average velocity of the Kuksai Glacier along the centerline in 2015–2016. (a) Monthly average velocity along the centerline in 2015–2016. (b) Monthly average velocity during 2015–2016.

The data from the Taxkogan meteorological station showed precipitation fluctuations throughout the year, with the highest precipitation from May to September. The temperature increased from January to July, and then decreased each month.

The high precipitation from May to September caused glacier mass accumulation. An increase in temperature in June and July resulted in glacier mass melting. The surface glacier velocity was the highest in June (figure in Section 4.4.2, $0.1836 \text{ m} \cdot \text{d}^{-1}$). However, the temperature and precipitation were high and low during July, respectively, decreasing the velocity ($0.125 \text{ m} \cdot \text{d}^{-1}$).

4.4.2. Kuokuosele Glacier

As shown in Figure 8b, the velocity of the Kuokuosele Glacier was the lowest at the end of the glacier and accelerated at about 3500 m from the end (altitude of about 4877 m). The glacier moved slightly faster along the centerline in May, June, and August ($0.088 \text{ m}\cdot\text{d}^{-1}$, $0.091 \text{ m}\cdot\text{d}^{-1}$, and $0.089 \text{ m}\cdot\text{d}^{-1}$, respectively). Figure 9b–d indicates that the change in the intra-annual velocity of the Kuokuosele Glacier was consistent with the increase and decrease in precipitation. As the temperature and precipitation increased from May to June, the glacier velocity increased from 0.088 to $0.091 \text{ m}\cdot\text{d}^{-1}$. The temperature and precipitation were significantly higher in August, and the glacier velocity was the highest at this time ($0.10 \text{ m}\cdot\text{d}^{-1}$). The temperature decreased from September to October, but September still had relatively high precipitation; thus, the glacier velocity accelerated in the subsequent months to 0.080 – $0.089 \text{ m}\cdot\text{d}^{-1}$. It was speculated that an increase in temperature caused glacier melting and accelerated the glacier velocity, but the precipitation had a more significant impact on glacier velocity than the temperature.

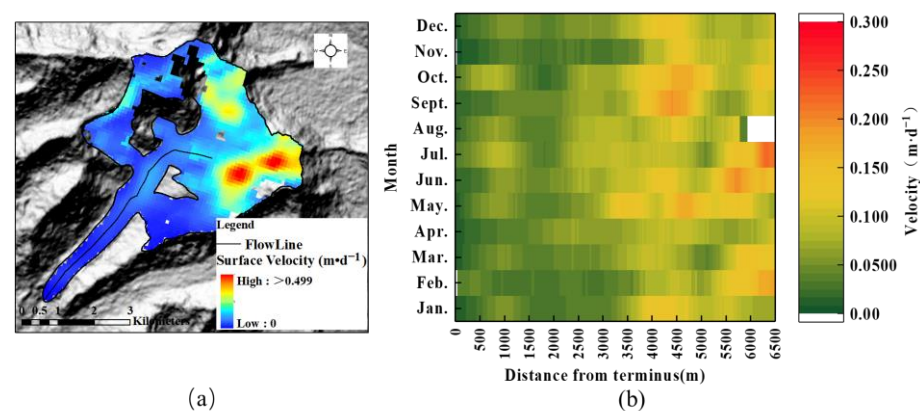


Figure 8. Changes in the monthly average velocity of the Kuokuosele Glacier along the centerline in 2015–2016. (a) Monthly average velocity along the centerline in 2015–2016. (b) Monthly average velocity during 2015–2016.

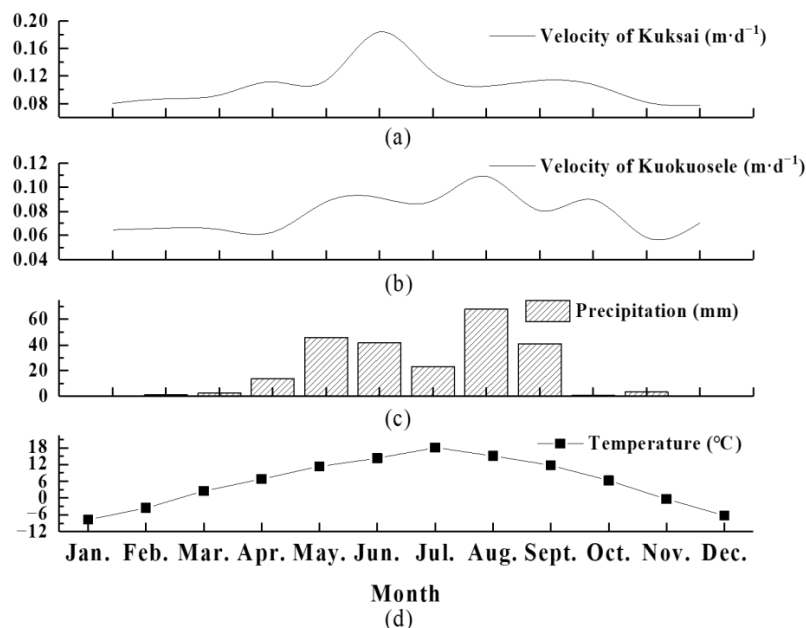


Figure 9. Changes in the velocity, precipitation, and average temperature of the Kuksai and Kuokuosele glaciers from 2015 to 2016. (a) Changes in the intra-annual velocity of the Kuksai Glacier; (b) changes in the intra-annual velocity of the Kuokuosele Glacier; (c) average monthly precipitation from 2015 to 2016; (d) average daily temperature from 2015 to 2016.

5. Discussion

In addition to temperature and precipitation, we also considered the effects of local morphological factors on glacier velocity. Table 2 indicates that the glacier velocity was generally higher on the western slopes (W/SW/NW) than on the eastern slopes (E/SE/NE) from 2013 to 2021. The velocity was more heterogeneous on the western slope (W) (STDV of $0.0147 \text{ m} \cdot \text{d}^{-1}$). Therefore, a linear regression analysis was used to calculate the correlation between annual average velocity and local morphological factors (area, length, slope, debris cover, and median elevation), except on the western slope.

Figure 10 shows the results of the linear regression analysis between glacier velocity and local morphological factors in the Muztag-Kongur Mountains from 2013 to 2021 (the confidence level was 95%). The results showed that the glacier velocity was moderately positively correlated with glacier area size ($R = 0.648$, $p = 0.001 < 0.05$) and glacier length ($R = 0.675$, $p = 0.001 < 0.05$). There was a weak correlation between glacier velocity and the mean slope ($R = 0.366$, $p = 0.072 > 0.05$), but no correlation between glacier velocity and debris cover ($R = 0.126$, $p = 0.547 > 0.05$) and between glacier velocity and median elevation ($R = -0.055$, $p = 0.792 > 0.05$).

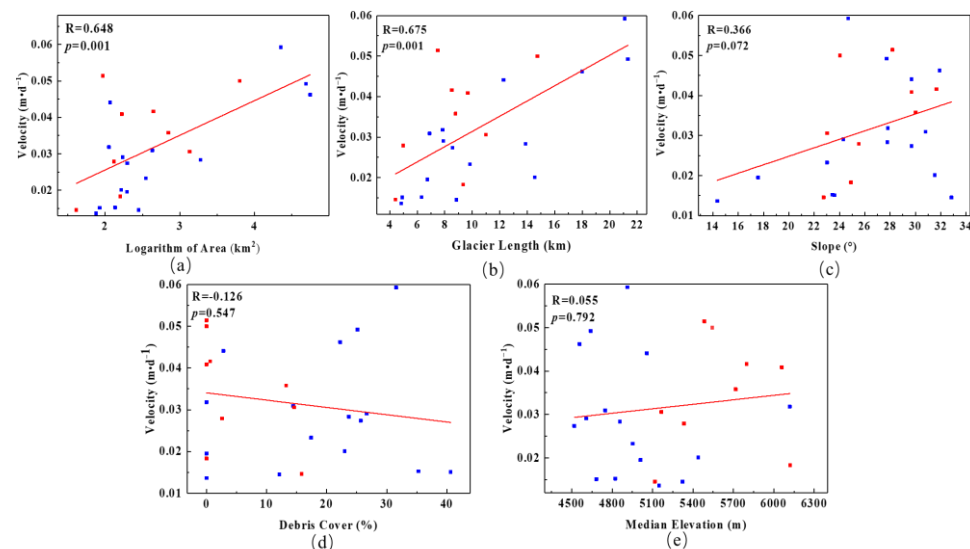


Figure 10. The results of linear regression analysis between glacier velocity and local morphological factors in the Muztag-Kongur Mountains: (a) logarithm of area; (b) length; (c) slope; (d) debris cover; (e) median elevation. The blue dots indicate glaciers on northern slopes, and the red dots indicate glaciers on southern slopes. R is the linear correlation coefficient between glacier velocity and local morphological factors, and p is the strength of the correlation.

Studies have shown that surface debris cover affects glacier velocity. Twenty-five of the glaciers were covered by debris, with a debris cover rate of 0.6% to 40.6%. Some studies have shown that debris cover can affect glacier melting [5,12,46]. For example, a study of the Muztag Glacier showed that surface debris of sufficient thickness inhibited glacier melting [45]. The stagnant glaciers typically had a 40% debris-covered area of the surface [47]. When the debris thickness was less than a critical value (about 20–30 cm), it promoted glacier melting [48]. The albedo of the debris layer is much lower than that of the ice and snow surface; thus, solar radiation causes more melting in debris-covered areas. The debris layer receives heat and transmits it to the glacier body, causing melting and accelerating the glacier movement [47,49]. A certain thickness of the debris will form a heat insulation layer on the glacier surface, which will block the heat absorption of the ice layer, thereby inhibiting glacier movement and eventually causing a decrease in glacier velocity [50]. Our results indicated no correlation between debris cover and glacier velocity ($R = 0.126$, $p = 0.547 > 0.05$), suggesting complex effects of the surface debris cover on glacier velocity. Studies have shown that the formation of debris cover may be related

to the slope ($>25^\circ$). The thickness of the debris layer affects the response of glaciers to climate warming [51]. Therefore, the effect of topography or climate should be considered in velocity studies of glaciers covered by debris.

As shown in Figure 11, the number and area of glaciers were larger on the western slopes than on the other slopes. Apart from the three maximum area glaciers (Karayalak, Qimugan, and Kuksai), glaciers on the western slopes (W/NW/SW) were generally larger than those on other slopes. The NW–SE trend of the Muztag-Kongur Mountains divides glaciers into windward and leeward glaciers [45]. This region is strongly affected by mid-altitude westerlies [6,45,52]. In recent years, enhancement of the westerlies has resulted in the mass accumulation of glaciers located on the windward slope. Therefore, the glaciers are larger on the western slope (their average area is 12.67 km^2). Because larger glaciers move faster, the glacier velocity was generally higher on western slopes than on other slopes.

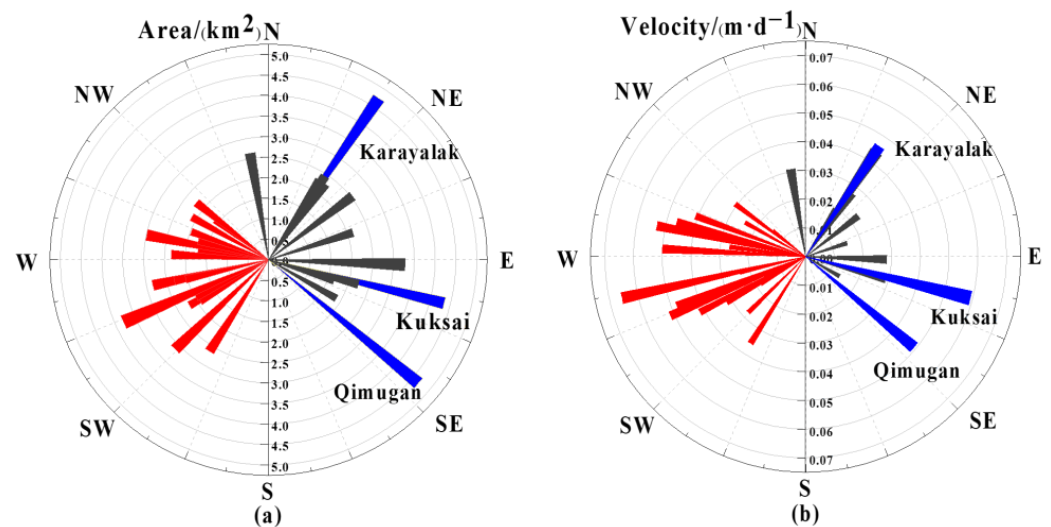


Figure 11. Glacier area and velocity in different slope directions: (a) area; (b) velocity. The red stripes represent glaciers on the western slope. The gray bands represent glaciers on the other slopes. The blue bands are the three largest glaciers in the Muztag-Kongur Mountains.

6. Conclusions

The COSI-Corr software was used to obtain the inter-annual velocity of glaciers in the Muztag-Kongur Mountains from 1990 to 2021 using Landsat time-series data and frequency-domain cross-correlation. The velocity trend of the Muztag-Kongur glaciers was analyzed in detail. The following conclusions were drawn:

- (1) The glacier velocity in the Muztag-Kongur Mountains has increased since 1990, and the peak velocity occurred in 1996/97. A transverse profile of two typical glaciers was used to analyze the monthly variation in glacier velocity during the year. The peaks of the monthly velocity of the two glaciers occurred in May and August. Since 1990, the inter-annual precipitation has increased, and the temperature changes slowed down from 2000 to 2013. The peak velocity occurred in 1996/97 due to increased precipitation in 1995. The fluctuations in the monthly velocities corresponded to the monthly precipitation trends. It has been speculated that high precipitation causes glacier mass accumulation; as the temperature rises, the glacier surface melts, and the velocity increases, so the precipitation has a more significant impact on glacier velocity than the temperature.
- (2) In addition to temperature and precipitation, the change in glacier velocity was moderately positively correlated with the glacier area size ($R = 0.648$, $p = 0.001 < 0.05$) and glacier length ($R = 0.675$, $p = 0.001 < 0.05$), and weakly correlated with the slope. There was a weak correlation between glacier velocity and the mean slope ($R = 0.366$, $p = 0.072 > 0.05$).

- (3) The glaciers had higher velocity and exhibited heterogeneity on the western slopes compared to the other slopes due to the westerly circulation, which causes the glaciers on the western slopes to become larger. Larger glaciers move faster, which explains the high velocities of the western slope glaciers.

In summary, long-term glacier velocity variation research of the Muztag-Kongur Mountains will contribute to a better understanding of glacier dynamics within the context of climatic warming.

Author Contributions: Conceptualization, L.J. and Z.Z.; methodology, D.H. and R.Z.; formal analysis, Y.L. and X.H.; data curation, D.H. and Y.L.; writing—original draft preparation, D.H.; writing—review and editing, R.Z., A.S. and Z.Z.; supervision, L.J. All authors have read and agreed to the published version of the manuscript.

Funding: This research was jointly funded by the National Natural Science Foundation of China (Grant Nos. 42071085, 41701087), the University-level general research project of Chuzhou University (Grant No. 2022XJYB03), the Academic Foundation for Top Talents in Disciplines of Anhui Universities (No. gxbjZD2022069), the Project of Natural Science Research of Anhui Provincial Department of Education (No. 2022AH030112, No. 2022AH040156) and the Innovation Program for Returned Overseas Chinese Scholars of Anhui Province (No. 2021LCX014).

Data Availability Statement: The data produced within this study are available in open repositories (Science Data Bank: <https://www.scidb.cn/en/detail?dataSetId=802608485131878400>, accessed on 10 October 2021), or are available from the authors upon request.

Acknowledgments: We thank the USGS for freely providing Landsat data and ASTER GDEM V2 data. We thank the NASA for providing ITS_LIVE data (<https://its-live.jpl.nasa.gov/>, accessed on 17 September 2019).

Conflicts of Interest: The authors declare no conflict of interest.

References

1. Stocker, T.; Boschung, J.; Qin, D.; Bex, V.; Midgley, P.; Tignor, M.; Plattner, G.-K.; Allen, S.; Xia, Y.; Nauels, A. *Climate Change 2013: The Physical Science Basis. Contribution of Working Group I to the Fifth Assessment Report of the Intergovernmental Panel on Climate Change*; Cambridge University Press: Cambridge, UK, 2013.
2. Xie, Z.; Liu, C. *Introduction to Glaciology*; Shanghai Popular Science Press: Shanghai, China, 2010.
3. Zhao, J.; Zhang, Z.; Xu, Y.; Wang, R.; Jiang, Z. Interannual and seasonal variation of flow velocity in Koxkar BaXi Glacier from 2014 to 2020. *J. Glaciol. Geocryol.* **2021**, *13*, 774.
4. Zhang, Z.; Huang, D.; Lu, Y.; Zhang, S. A Landsat-based dataset of glacier velocity in Eastern Pamir from 1989 to 2020. *China Sci. Data.* **2021**, *6*, 170–181. [[CrossRef](#)]
5. Paul, F.; Bolch, T.; Kääb, A.; Nagler, T.; Nuth, C.; Scharrer, K.; Shepherd, A.; Strozzi, T.; Ticconi, F.; Bhambri, R.; et al. The glaciers climate change initiative: Methods for creating glacier area, elevation change and velocity products. *Remote Sens. Environ.* **2015**, *162*, 408–426. [[CrossRef](#)]
6. Yan, S.; Guo, H.; Liu, G.; Fu, W. Monitoring Muztagh Kuksai Glacier surface velocity with L-band SAR data in southwestern Xinjiang, China. *Environ. Earth Sci.* **2013**, *70*, 3175–3184. [[CrossRef](#)]
7. Yasuda, T.; Furuya, M. Dynamics of surge-type glaciers in West Kunlun Shan, Northwestern Tibet. *J. Geophys. Res. Earth Surf.* **2015**, *120*, 2393–2405. [[CrossRef](#)]
8. Karimi, N.; Farokhnia, A.; Shishangosht, S.; Elmi, M.; Eftekhari, M.; Ghalkhani, H. Elevation changes of Alamkouh Glacier in Iran since 1955, based on remote sensing data. *Int. J. Appl. Earth Obs. Geoinf.* **2012**, *19*, 45–58. [[CrossRef](#)]
9. Guan, W.; Cao, B.; Pan, B. Research of glacier flow velocity: Current situation and prospects. *J. Glaciol. Geocryol.* **2020**, *42*, 1101–1114. [[CrossRef](#)]
10. Zhou, J.; Li, Z.; Guo, W. Estimation and analysis of the surface velocity field of mountain glaciers in Muztagata using satellite SAR data. *Environ. Earth Sci.* **2013**, *71*, 3581–3592. [[CrossRef](#)]
11. Wang, Q. *Application of DInSAR and Offset Tracking Technology in Velocity Monitoring of Mountain Glaciers*; China University of Geosciences: Beijing, China, 2018.
12. Berthier, E.; Vadon, H.; Baratoux, D.; Arnaud, Y.; Vincent, C.; Feigl, K.L.; Remy, F.; Legresy, B. Surface motion of mountain glaciers derived from satellite optical imagery. *Remote Sens. Environ.* **2005**, *95*, 14–28. [[CrossRef](#)]
13. Brun, F.; Berthier, E.; Wagnon, P.; Kääb, A.; Treichler, D. A spatially resolved estimate of High Mountain Asia glacier mass balances from 2000 to 2016. *Nat. Geosci.* **2017**, *10*, 668–673. [[CrossRef](#)]
14. Gardelle, J.; Berthier, E.; Arnaud, Y.; Kääb, A. Region-wide glacier mass balances over the Pamir-Karakoram-Himalaya during 1999–2011. *Cryosphere* **2013**, *7*, 1263–1286. [[CrossRef](#)]

15. Treichler, D.; Kääb, A.; Salzmann, N.; Xu, C. Recent glacier and lake changes in High Mountain Asia and their relation to precipitation changes. *Cryosphere* **2019**, *13*, 2977–3005. [\[CrossRef\]](#)
16. Hewitt, K. The Karakoram anomaly? Glacier expansion and the “elevation effect” Karakoram Himalaya. *Mt. Res. Dev.* **2005**, *25*, 332–340. [\[CrossRef\]](#)
17. Lv, M.; Quincey, D.; Guo, H.; King, O.; Liu, G.; Yan, S.; Lu, X.; Ruan, Z. Examining geodetic glacier mass balance in the eastern Pamir transition zone. *J. Glaciol.* **2020**, *66*, 927–937. [\[CrossRef\]](#)
18. Zhang, Z.; Liu, S.; Wei, J.; Xu, J.; Guo, W.; Bao, W.; Jiang, Z. Mass Change of Glaciers in Muztagh Ata-Kongur Tagh, Eastern Pamir, China from 1971/76 to 2013/14 as Derived from Remote Sensing Data. *PLoS ONE* **2016**, *11*, e0147327. [\[CrossRef\]](#)
19. Yao, T.; Thompson, L.; Yang, W.; Yu, W.; Gao, Y.; Guo, X.; Yang, X.; Duan, K.; Zhao, H.; Xu, B. Different glacier status with atmospheric circulations in Tibetan Plateau and surroundings. *Nat. Clim. Chang.* **2012**, *2*, 663–667. [\[CrossRef\]](#)
20. Zhang, Z.; Xu, J.; Liu, S.; Guo, W.; Wei, J.; Feng, T. Glacier changes since the early 1960s, eastern Pamir, China. *J. Mt. Sci.* **2016**, *13*, 276–291. [\[CrossRef\]](#)
21. Dehecq, A.; Gourmelen, N.; Gardner, A.S.; Brun, F.; Goldberg, D.; Nienow, P.W.; Berthier, E.; Vincent, C.; Wagnon, P.; Trounev, E. Twenty-first century glacier slowdown driven by mass loss in High Mountain Asia. *Nat. Geosci.* **2019**, *12*, 22–27. [\[CrossRef\]](#)
22. Jiang, Z.; Liu, S.; Long, S.; Lin, J.; Wang, X.; Li, J.; Xu, J.; Wei, J.; Bao, W. Analysis of the glacier dynamics features in Kongur Mountain based on SAR technology and DEMs. *J. Glaciol. Geocryol.* **2014**, *36*, 286–295. [\[CrossRef\]](#)
23. Yang, H.; Yan, S.; Liu, G.; Ruan, Z. Fluctuations and movements of the Kuksai Glacier, western China, derived from Landsat image sequences. *J. Appl. Remote Sens.* **2013**, *8*, 084599. [\[CrossRef\]](#)
24. Yan, S.; Li, Y.; Ruan, Z.; Lv, M.; Liu, G.; Deng, K. Wavelet-Based Topographic Effect Compensation in Accurate Mountain Glacier Velocity Extraction: A Case Study of the Muztagh Ata Region, Eastern Pamir. *Remote Sens.* **2017**, *9*, 697. [\[CrossRef\]](#)
25. Lv, M.; Guo, H.; Lu, X.; Liu, G.; Yan, S.; Ruan, Z.; Ding, Y.; Quincey, D. Characterizing the behaviour of surge- and non-surge-type glaciers in the Kingata Mountains, eastern Pamir, from 1999 to 2016. *Cryosphere* **2019**, *13*, 219–236. [\[CrossRef\]](#)
26. Shangguan, D.; Liu, S.; Ding, Y.; Gou, W.; Xu, B.; Xu, J.; Jiang, Z. Characterizing the May 2015 Karayaylak Glacier surge in the eastern Pamir Plateau using remote sensing. *J. Glaciol.* **2016**, *62*, 944–953. [\[CrossRef\]](#)
27. Yao, X.; Iqbal, J.; Li, L.-J.; Zhou, Z.-K. Characteristics of mountain glacier surge hazard: Learning from a surge event in NE Pamir, China. *J. Mt. Sci.* **2019**, *16*, 1515–1533. [\[CrossRef\]](#)
28. Zhang, Z.; Tao, P.; Liu, S.; Zhang, S.; Huang, D.; Hu, K.; Lu, Y. What controls the surging of Karayaylak glacier in eastern Pamir? New insights from remote sensing data. *J. Hydrol.* **2022**, *607*, 127577. [\[CrossRef\]](#)
29. Zhang, Z. Mass changes of glaciers in eastern Pamir using remote sensing and GIS. *Acta Geod. Cartogr. Sin.* **2021**, *50*, 992. [\[CrossRef\]](#)
30. Liu, S.; Yao, X.; Guo, W.; Xu, J. The contemporary glaciers in China based on the Second Chinese Glacier Inventory. *Acta Geogr. Sin.* **2015**, *70*, 13–16. [\[CrossRef\]](#)
31. Wang, L.; Jiang, Z.; Liu, S.; Zhang, Z. Dataset of glacier surface motion along KKH during 2015–2017. *China Sci. Data.* **2018**, *9*, 72–81. [\[CrossRef\]](#)
32. Guo, W.; Liu, S.; Xu, J.; Wei, J.; Ding, L. Monitoring recent surging of the Yulinchuan glacier on north slopes of Muztagh Range by remote sensing. *J. Glaciol. Geocryol.* **2012**, *34*, 765–774. [\[CrossRef\]](#)
33. Sun, Y. *Spatial-Temporal Characteristics of Changes in Glacier Velocity at the Karakoram in the Past 30 Years and Its Influence Factors*; Institute of Geodesy and Geophysics, Chinese Academy of Sciences: Wuhan, China, 2018.
34. Sun, Y.; Jiang, L.; Liu, L.; Sun, Y.; Wang, H. Spatial-Temporal Characteristics of Glacier Velocity in the Central Karakoram Revealed with 1999–2003 Landsat-7 ETM+ Pan Images. *Remote Sens.* **2017**, *9*, 1064. [\[CrossRef\]](#)
35. Sam, L.; Bhardwaj, A.; Kumar, R.; Buchroithner, M.F.; Martín-Torres, F.J. Heterogeneity in topographic control on velocities of Western Himalayan glaciers. *Sci. Rep.* **2018**, *8*, 12843. [\[CrossRef\]](#) [\[PubMed\]](#)
36. Gardner, A.S.; Fahnestock, M.; Scambos, T. *Update to Time of Data Download: ITS_LIVE Regional Glacier and Ice Sheet Surface Velocities*; National Snow and Ice Data Center: Boulder, CO, USA, 2019. [\[CrossRef\]](#)
37. Gardner, A.S.; Moholdt, G.; Scambos, T.; Fahnestock, M.; Ligtenberg, S.; van den Broeke, M.; Nilsson, J. Increased West Antarctic and unchanged East Antarctic ice discharge over the last 7 years. *Cryosphere* **2018**, *12*, 521–547. [\[CrossRef\]](#)
38. Wang, L.; Jiang, Z.; Liu, S.; Shangguan, D.; Zhang, Y. Characteristic of Glaciers’ Movement Along Karakoram Highway. *Remote Sens. Tech Applic.* **2019**, *34*, 412–423. [\[CrossRef\]](#)
39. Arendt, A.; Bliss, A.; Bolch, T.; Cogley, J.; Gardner, A.; Hagen, J.-O.; Hock, R.; Huss, M.; Kaser, G.; Kienholz, C. *Randolph Glacier Inventory—A Dataset of Global Glacier Outlines: Version 6.0: Technical Report, Global Land Ice Measurements from Space*; RGI Consortium: Boulder, CO, USA, 2017. [\[CrossRef\]](#)
40. Ayoub, F.; Leprince, S.; Avouac, J. *User’s Guide to Cosi-Corr*; California Institute of Technology: Pasadena, CA, USA, 2015.
41. Yao, X.; Liu, S.; Zhu, Y.; Gong, P.; An, L.; Li, X. Design and implementation of an automatic method for deriving glacier centerlines based on GIS. *J. Glaciol. Geocryol.* **2015**, *37*, 1563–1570. [\[CrossRef\]](#)
42. Zhang, D.; Yao, X.; Duan, H.; Liu, S.; Guo, W.; Sun, M.; Li, D. A new automatic approach for extracting glacier centerlines based on Euclidean allocation. *Cryosphere* **2021**, *15*, 1955–1973. [\[CrossRef\]](#)
43. Bolch, T.; Pieczonka, T.; Benn, D.I. Multi-decadal mass loss of glaciers in the Everest area (Nepal Himalaya) derived from stereo imagery. *Cryosphere* **2011**, *5*, 349–358. [\[CrossRef\]](#)

44. Koblet, T.; Gärtner-Roer, I.; Zemp, M.; Jansson, P.; Thee, P.; Haeberli, W.; Holmlund, P. Reanalysis of multi-temporal aerial images of Storglaciären, Sweden (1959–99)—Part 1 Determination of length, area, and volume changes. *Cryosphere* **2010**, *4*, 333–343. [[CrossRef](#)]
45. Holzer, N.; Vijay, S.; Yao, T.; Xu, B.; Buchroithner, M.; Bolch, T. Four decades of glacier variations at Muztagh Ata (eastern Pamir): A multi-sensor study including Hexagon KH-9 and Pléiades data. *Cryosphere* **2015**, *9*, 2071–2088. [[CrossRef](#)]
46. Song, C.; Sheng, Y.; Wang, J.; Ke, L.; Madson, A.; Nie, Y. Heterogeneous glacial lake changes and links of lake expansions to the rapid thinning of adjacent glacier termini in the Himalayas. *Geomorphology* **2016**, *280*, 30–38. [[CrossRef](#)]
47. Scherler, D.; Bookhagen, B.; Strecker, M.R. Spatially variable response of Himalayan glaciers to climate change affected by debris cover. *Nat. Geosci.* **2011**, *4*, 156–159. [[CrossRef](#)]
48. Zhang, Y.; Liu, S. Research progress on debris thickness estimation and its effect on debris-covered glaciers in western China. *Acta Geogr. Sin.* **2017**, *72*, 1606–1620. [[CrossRef](#)]
49. Shrestha, A.B.; Aryal, R. Climate change in Nepal and its impact on Himalayan glaciers. *Reg. Environ. Chang.* **2010**, *11*, 65–77. [[CrossRef](#)]
50. Rounce, D.R.; McKinney, D.C. Thermal resistances in the Everest Area (Nepal Himalaya) derived from satellite imagery using a nonlinear energy balance model. *Cryosphere Discuss.* **2014**, *8*, 887–918. [[CrossRef](#)]
51. Ogilvie, I.H. The effect of superglacial debris on the advance and retreat of some Canadian glaciers. *J. Geol.* **1904**, *12*, 722–743. [[CrossRef](#)]
52. Seong, Y.B.; Owen, L.A.; Yi, C.; Finkel, R.C.; Schoenbohm, L. Geomorphology of anomalously high glaciated mountains at the northwestern end of Tibet: Muztagh Ata and Kongur Shan. *Geomorphology* **2009**, *103*, 227–250. [[CrossRef](#)]

Disclaimer/Publisher’s Note: The statements, opinions and data contained in all publications are solely those of the individual author(s) and contributor(s) and not of MDPI and/or the editor(s). MDPI and/or the editor(s) disclaim responsibility for any injury to people or property resulting from any ideas, methods, instructions or products referred to in the content.